Dinitrogen as a universal electron acceptor in solid-state chemistry: an example of uncommon metallic compounds $Na_3(N_2)_4$ and NaN_2

Maxim Bykov,[a,b,*] Kelin R. Tasca,[a,b] Iskander G. Batyrev,[c] Dean Smith,[d] Konstantin Glazyrin,[e] Stella Chariton,[f] Mohammad Mahmood,[a] Alexander F. Goncharov[b]

[a] Department of Mathematics, Howard University, Washington, DC 20059, USA

[b] The Earth and Planets Laboratory, Carnegie Institution for Science, Washington, DC 20015, USA

[c] U.S. Army Research Laboratory, RDRL-WML-B, Aberdeen Proving Ground Maryland, 21005 USA

[d] HPCAT, X-ray Science Division, Argonne National Laboratory, Argonne, IL 60439, USA

[e] Photon Science, Deutsches Elektronen-Synchrotron, 22607 Hamburg, Germany

[f] Center for Advanced Radiation Sources, University of Chicago, Lemont, IL 60437, USA

ABSTRACT: With the exception of Li, alkali metals do not react with elemental nitrogen neither at ambient conditions nor at elevated temperatures, requiring the search for alternative synthetic routes to their nitrogen-containing compounds. Here using a controlled decomposition of sodium azide NaN_3 at high pressure conditions we synthesize two novel compounds $Na_3(N_2)_4$ and NaN_2 both containing dinitrogen anions. NaN_2 synthesized at 4 GPa might be the common intermediate in high-pressure solid-state metathesis reactions where NaN_3 is used as a source of nitrogen, while $Na_3(N_2)_4$ opens a new class of compounds, where $[N_2]$ units accommodate a non-integer formal charge of -0.75. This finding can dramatically extend the expected compositions in other group 1-2 metal-nitrogen systems. Electronic structure calculations show the metallic character for both compounds.

KEYWORDS: High-pressure chemistry, diazenides, nitrogen, nitrides, sodium azide, azides, pernitride, nitrogen fixation

Introduction

Homonuclear dinitrogen anions are common intermediates in biological and organo-metallic synthetic chemistry, and play an important role in the processes of nitrogen reduction to ammonia.[1–3] In extended solid state compounds, nitrogen typically present in a form of a nitride anion N^{3-} and does not form catenated polyanions (with the exception of azides). The first alkaline-earth diazenides SrN, SrN_2 and BaN_2 containing $[N_2]^{2-}$ anions were synthesized from elements at high-pressure conditions only in the early 2000s.[4,5] Later Schnick *et al*. used controlled decomposition of alkali and alkaline-earth metal azides at 3-12 GPa to obtain diazenides Li_2N_2, CaN_2, SrN_2 and BaN_2.[6,7] Diamond anvil cell techniques allowed the synthesis of a series of transition-metal compounds MN_2 (M = Ti, Cr, Fe, Co, Ni, Cu, Ru, Rh, Pd, Re, Os, Ir, Pt) at pressures 30-70 GPa.[8–17] Further pressure increase leads to extended nitrogen catenation and formation of various polynitrogen species such as polytetrazene $[-N-N-N=N-]_n$ in FeN_4 and Hf_2N_{11},[18–20] polyacetylene-like chains in MgN_4,[21] $Hf_4N_{20}{\cdot}N_2$, $WN_8{\cdot}N_2$, $Os_5N_{28}{\cdot}3N_2$,[20] $ReN_8{\cdot}N_2$,[22] pentazolate *cyclo*-N_5^- in CsN_5[23] and LiN_5.[24]

In MN_2 compounds metals usually possess their common oxidation states, while dinitrogen anion formally accommodates from 1 to 4 electrons. The degree of the charge transfer from metal to nitrogen significantly affects the properties of materials. For example, pernitrides of Pt, Ir, Os, Ti with $[N_2]^{4-}$ units and metals in the oxidation state IV are much more incompressible than $M^{III}N_2$ (M = Cr, Fe, Co, Ni, Ru, Rh) with $[N_2]^{3-}$, diazenides $M^{II}N_2$ (M = Ca, Ba, Sr) with $[N_2]^{2-}$ and $M^{I}N_2$ (M = Li, Cu) with $[N_2]^{-}$.

Despite a very wide range of metals with extremely different properties the stoichiometry of their compounds containing exclusively $[N_2]^{x-}$ anions is always MN_2 with the exception of recently-synthesized lithium diazenide Li_2N_2.[7] Here we synthesize two novel compounds in the Na-N system: NaN_2 at ~4 GPa and a compound with an unusual composition $Na_3(N_2)_4$ at ~28 GPa containing $[N_2]$ units with non-integer formal charge of -0.75. $Na_3(N_2)_4$ opens a new class of $[N_2]$ – containing compounds with variable stoichiometry.

The most common high-pressure route to nitrogen-rich compounds is a direct reaction between metal and nitrogen in a laser-heated diamond anvil cell. However, this method has disadvantages such as inherent inhomogeneity of the reaction mixture with varying metal: nitrogen ratio across the sample. The use of azides as precursors offers a solution to this problem. Furthermore, azides provide a nitrogen-rich environment with $N/M \geq 3$, and this nitrogen is already activated, *i.e.* the activation barrier for the reaction is usually lower than in the reaction of metal with the triply bound N_2 molecule.

Sodium azide NaN_3 was an object of many high-pressure studies primarily due to its application as a high energy density material. Structural studies of NaN_3 at high pressures are challenging since the compound loses its crystallinity on compression. There are at least three structurally characterized phases of sodium azide: α-NaN_3 (*C*2/*m*), ß-NaN_3 (*R*-3*m*) and γ-NaN_3 (*I*4/*mcm*).[25] Two high-pressure phases above 18 and 29 GPa were observed by Zhu *et al*. using XRD,[26] but the structures were not determined. High-pressure Raman spectroscopy studies by Eremets *et al*.[27] suggested the transformation of azide anions to larger nitrogen clusters in compressed NaN_3, however structural characterization of these transitions is missing. Based on *ab initio* calculations Zhang *et al*. suggested that azide anions in compressed NaN_3 would condense to hexazine N_6 rings above 58 GPa.[28] Peiris *et al*.[29] and Holtgrewe *et al*.[30] demonstrated that photolysis of NaN_3 leads to the formation of non-crystalline products. Here we established an alternative route for synthesis of Na-N compounds from sodium azide by infrared laser heating at high pressure in diamond anvil cells.

Experimental section

Samples preparation

The high-pressure high-temperature behavior of NaN_3 (99.5%, Sigma-Aldrich) was studied on three samples. For single-crystal XRD studies (samples #1 and #2), a powder of sodium azide NaN_3 was placed in a sample chamber of a BX90 diamond anvil cell equipped with Boehler-Almax type diamonds.[31,32] Re foil preindented to a thickness of 30 μm served as a gasket. A ruby chip was placed inside the sample chamber for pressure measurement. Sample #3 in a symmetric diamond anvil cell and with standard-cut diamonds was used for additional Raman measurements. The samples were compressed up to 26 (Sample #1), 4 GPa (Sample #2) and 25 GPa (Sample #3) and laser-heated (λ = 1064 nm) using double-sided laser-heating systems of the beamlines P02.2 (Petra III, DESY, Hamburg, Germany)[33], HPCAT (APS, Argonne, USA) and GSECARS (APS, Argonne, USA) respectively. No pressure-transmitting medium was used in all experiments. For samples #1 and #2, it was not possible to get the precise temperature of laser-heating, because the thermal radiation emitted by the sample was very weak. From the brightness of the heating spot, the temperature can be estimated to be below 1000 K. The sample #3 was heated up to ~1900(200) K as determined by the black body radiation fit.

X-ray diffraction

XRD measurements of the sample #1 were performed at the beamline P02.2 of Petra III (DESY, Hamburg, Germany) with the X-ray beam (λ = 0.2891 Å) focused down to 1.8×2 μm² by a Kirkpatrick-Baez mirror system and diffraction patterns were collected on a PerkinElmer XRD 1621 flat-panel detector. XRD measurements of the sample #2 were performed at the beamline 16ID-B (APS, Argonne, USA) with the X-ray beam (λ = 0.4066 Å) focused down to 5×5 μm² by a Kirkpatrick-Baez mirror system and diffraction patterns were collected on a Pilatus 1M detector. XRD measurements of the sample #3 were performed at the beamline 13IDD (GSECARS, APS, Argonne, USA) with the X-ray beam (λ = 0.2952 Å) focused down to 3×3 μm² by a Kirkpatrick-Baez mirror system and diffraction patterns were collected on a Pilatus 1M detector (CdTe). For the single-crystal XRD measurements samples were rotated around a vertical ω-axis in a range ±35°. The diffraction images were collected with an angular step Δω = 0.5° and an exposure time of 1s or 2s/frame. For the analysis of the single-crystal diffraction data (indexing, data integration, frame scaling and absorption correction) we used the *CrysAlis*^{Pro} software package. Specific details of the multigrain dataset analysis are given in the Supporting Information and in the Figure S1. To calibrate an instrumental model in the *CrysAlis*^{Pro} software, *i.e.*, the sample-to-detector distance, detector's origin, offsets of goniometer angles, and rotation of both X-ray beam and the detector around the instrument axis, we used a single crystal of orthoenstatite ($(Mg_{1.93}Fe_{0.06})(Si_{1.93}, Al_{0.06})O_6$, *Pbca* space group, a = 8.8117(2), b = 5.18320(10), and c = 18.2391(3) Å). Using the Olex2 crystallography software package, the structures were solved with the ShelXT structure solution program[34] using Intrinsic Phasing and refined with the ShelXL[35] refinement package using Least Squares minimization. The powder diffraction images were integrated to powder patterns with Dioptas software.[36] Le-Bail fits of the diffraction patterns were performed with the Jana2006 software.[37] CSD-1999694 and CSD-1999711 contain the supplementary crystallographic data for this paper. These data can be obtained free of charge from FIZ Karlsruhe *via* www.ccdc.cam.ac.uk/structures"

Raman spectroscopy

Raman spectra were measured using the GSECARS Raman system with the excitation wavelength of 532 nm. The full description of the Raman system has been published elsewhere.[38]

Theoretical calculations

The minimum enthalpy structures were recalculated with the norm conserving part of the PAW. [39] Energy cut-off of 750-830 eV using the density functional theory (DFT) code CASTEP [40] and exchange-correlation functional in Perdew-Burke-Ernzerhof (PBE) approximation.[41] Thirty irreducible k-points were used for electronic Brillouin zone integration and Tkachenko-Schefler dispersion correction was enabled [42]. The Brillouin zone integrals were performed using Monkhorst- Pack grids [43] with spacings between grid points of less than 0.01 $Å^{-1}$. The structures were considered converged when the force on each atom was less than 0.002 eV/Å and total energy tolerance was better than 10^{-7} eV. Deviation of the stress tensor from that defined by the target pressure was less than 0.001 GPa. The phonon dispersion and phonon frequencies calculations were performed using a finite displacements method implemented in CASTEP code.[44] Finite displacement phonons are calculated only at the commensurate q-points at the cost of creating a supercell. The population analysis was carried out as implemented in CASTEP.[45]

Results and discussion

The laser heating of NaN_3 at 26 GPa leads to an irreversible chemical reaction that is evidenced by the changes in the optical properties of the sample (heated area becomes opaque, see inset in Figure 1a). After the heating, the pressure increased up to ~28 GPa. The reaction product has a rich spotty diffraction pattern that allowed using single-crystal XRD analysis (Figure 1b, Table S1). The methodology of such multigrain analysis is described in a number of our recent publications (e.g., Ref. [15]). The diffraction pattern could be indexed with the tetragonal body-centered unit cell with a = 4.9597(16) and c = 16.29(7) Å. Successful structure solution was achieved in a space group $I4_1/amd$ (No. 141) and revealed the composition of the new compound as Na_3N_8. Full crystallographic information for this compound is provided in the Table S1 and in the supporting *cif* file. The expected decomposition reaction of NaN_3 should result in either the release of molecular nitrogen, or in the formation of polynitrides NaN_x with $x > 3$:

$$3NaN_3 \rightarrow Na_3N_8 + \frac{1}{2}N_2 \quad (1)$$

$$\frac{3x-8}{x-3}NaN_3 \rightarrow Na_3N_8 + \frac{1}{x-3}NaN_x \quad (2)$$

Experimental information on compounds NaN_x with $x > 3$ is limited to a Na-pentazolate framework MPF-1, which is not expected to form at high pressure due to its open zeolitic architecture.[46] However, recently Steele and Oleynik predicted that sodium pentazolate NaN_5 would be among thermodynamically stable phases in the Na-N system at elevated pressures.[47] In order to get an insight into the mechanism of NaN_3 decomposition, we have performed Raman spectroscopy measurements (Figures S2-S4). Although we could identify peaks corresponding to the nitrogen stretching vibration (ν_1 = 2376 cm^{-1} at ~12 GPa, Figure S2) there is an indication that some other nitrogen-containing phases may be present in the sample chamber (Figure S4). Therefore, both reactions 1 and 2 may take place. It is likely that nitrogen and products NaN_x might not be well crystallized, to produce strong diffraction peaks, which would allow their unambiguous XRD identification in a mixture with Na_3N_8. The reaction (1) is also supported by our theoretical calculations, suggesting that it is exothermic with ΔH = -0.261 eV per NaN_3 unit.

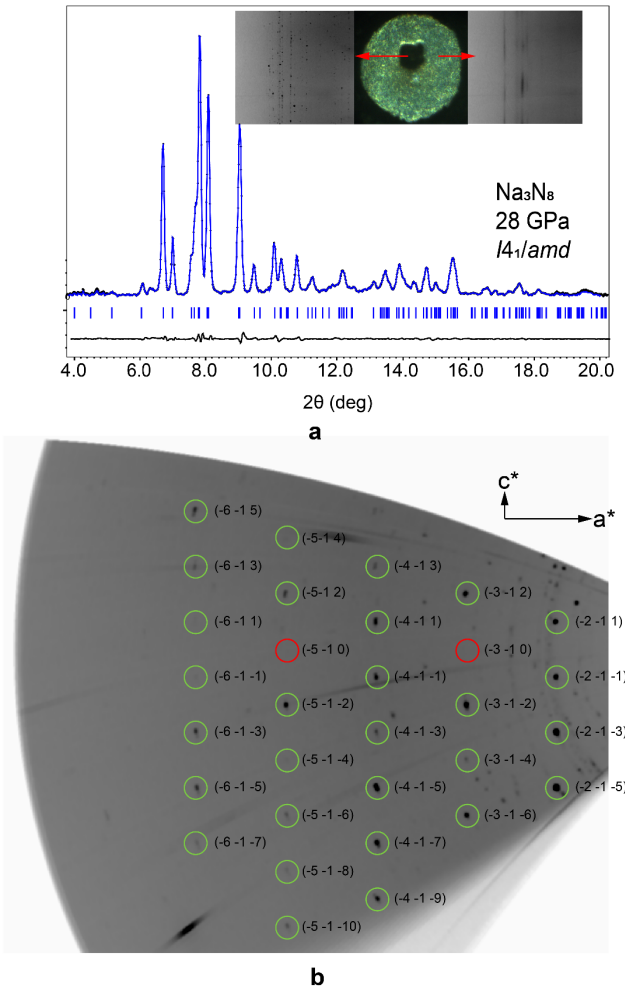

Figure 1. (a) Powder diffraction pattern of Na_3N_8 at ~28 GPa, λ = 0.2891 Å. Inset shows and optical image of the heated sample area at ~28 GPa and cake slices of the diffraction images of non-heated and heated sample areas (b) Reconstructed (*h*-1*l*) precession image from the single-crystal XRD dataset at 28 GPa. Reflections *hkl* with *h*+*k*+*l* = 2*n* +1 are absent due to the *I*-centering of the lattice. Reflections *hk*0 with *h* = 2*n*+1 or *k* = 2*n*+1 (marked by red circles) are absent due to the glide plane symmetry operations of the space group $I4_1/amd$.

Na_3N_8 has an unprecedented structure type. However, two symmetry-independent sodium atoms Na1 and Na2 occupying Wyckoff sites 4*a* and 8*e* respectively form a substructure isostructural to α-$ThSi_2$ (Figure 2a). Each Na2 atom has three close Na2 neighbors with *d*(Na-Na) = 2.81 and 2.78 Å at 28 GPa. These distances are close to those in *bcc*-Na at similar pressures (2.79 Å).[48] With Na2-Na2-Na2 angles close to 120°, Na2 atoms form one of the basic 3-connected three-dimensional nets (*ths*) described by a vertex symbol $10_210_410_4$.[49] Two nitrogen atoms N1 and N2 occupy Wyckoff sites 16*h* an 16*f* respectively and form N1-N1 and N2-N2 dinitrogen dumbbells with *d*(N1-N1) = 1.147(3) Å and *d*(N2-N2) = 1.149(3) Å at 28 GPa. N1-N1 units are surrounded by seven sodium atoms forming a distorted pentagonal bipyramid as shown in the Figures 2*b*-2*d*, while N2-N2 units are surrounded by six sodium atoms that form a distorted octahedron. Na1 atoms are coordinated by eight N_2 units in a side-on manner, while Na2 – by eight end-on N_2 and one side-on N_2 units. Side-on coordination usually leads to a greater charge transfer[50], which is in a good agreement with our calculations of Mulliken atomic charges (Table S2).

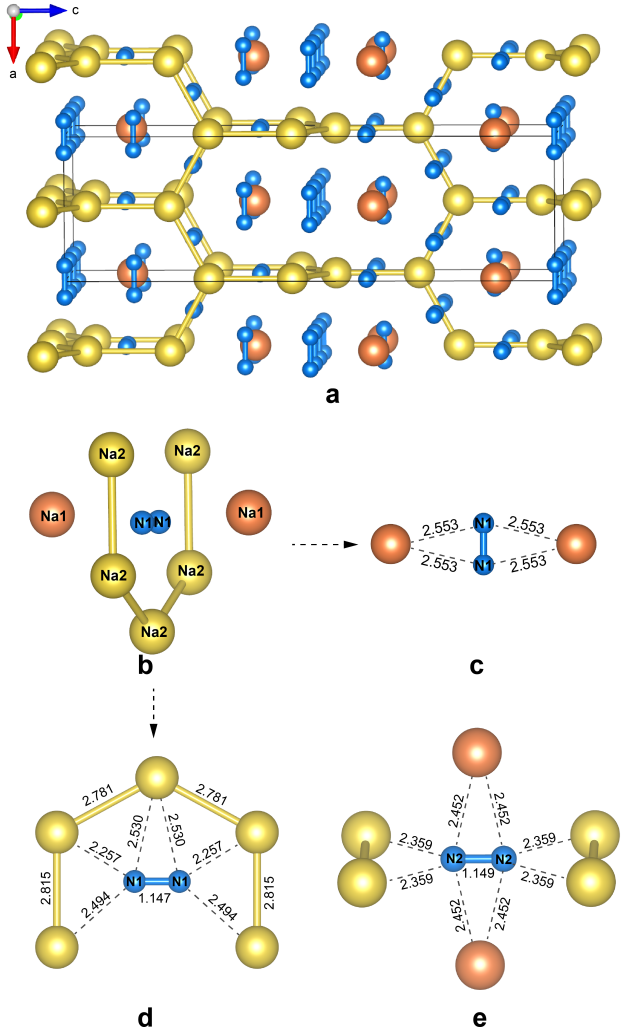

Figure 2. (a) Crystal structure of Na_3N_8 at 28 GPa. Shortest Na-Na contacts are indicated by yellow sticks (b)-(e) Coordination environments of nitrogen molecules.

To study the stability region of Na_3N_8 the sample was decompressed in a few steps to ambient pressure. Na_3N_8 remains in the sample chamber down to 7.7 GPa. Lattice parameters increase with decreasing pressure with *c*/*a* ratio approaching, but not reaching, the ideal value for the *ths* net of $2\sqrt{3}$. One can notice a slight kink in the pressure-dependence of the unit cell parameters *a* and *c* at ~15 GPa (Figure S5). We should note here that while the experiment was performed under very non-hydrostatic conditions the evolution of deviatoric stresses may influence the behavior of the lattice parameters on compression or decompression. Furthermore, the certain systematic error in pressure determination may occur due to the pressure gradient between the pressure marker (ruby) and the heated spot. However, we should also mention that the refined N1-N1 and N2-N2 distances that are similar above 15 GPa, begin to deviate at lower pressures (Figure S5). The N2-N2 distance unexpectedly decreases with decreasing pressure and tends to the N-N distance in triply bound dinitrogen molecule. This may indicate the onset of charge redistribution between two dinitrogen units and an onset of further decomposition.

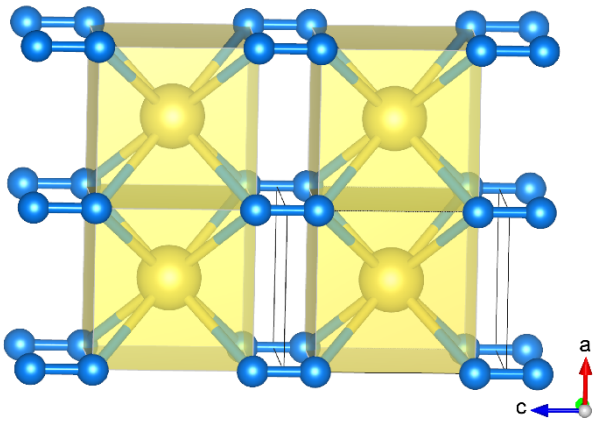

Figure 3. Crystal structure of NaN_2 at 4 GPa. Nitrogen and sodium atoms shown as blue and yellow spheres, respectively. NaN_8 coordination polyhedra are highlighted. *d*(N-N) = 1.161(9) Å, *d*(Na-N) = 2.582(3) Å.

Further decompression to 4 GPa resulted in the disappearance of all single-crystalline spots in the diffraction pattern and in the formation of a powder-like sample. Primitive tetragonal unit cell with *a* = 3.0009(13) and *c* = 4.101(3) Å describes the positions of the diffraction peaks with a good agreement (Figure S6). To recrystallize this compound, the sample was slightly heated by the infrared laser (λ = 1064 nm), which allowed the analysis of the crystal structure by means of single-crystal X-ray diffraction. Structure solution and refinement revealed the composition of this compound as NaN_2 (Table S1). NaN_2 is isostructural to α-$FeSi_2$ and has a space group *P*4/*mmm* (No. 123). It can be described as a layer packing structure, in which the layers are stacked along [001]. The layers consisting of face-sharing NaN_8 slightly distorted cubes are interconnected through N-N bonds with *d*(NN) = 1.161(9) Å at 4 GPa (Figure 3). Powder-like NaN_2 was also obtained in a separate experiment by heating sodium azide compressed at 4.5 GPa (Figure S6). On decompression NaN_2 is stable down to at least 2.8 GPa but decomposes with the formation of *bcc*-Na at ambient pressure (Figure S6).

Both Na_3N_8 and NaN_2 have very unusual electron counts. The chemical formula of Na_3N_8 can be rewritten as $Na_3(N_2)_4$ and if we assume that Na is in its standard oxidation state +I, the charge on each dinitrogen unit would be -0.75. Obviously, 0.75 electrons cannot be localized on the nitrogen antibonding π* orbitals and these electrons must be either delocalized, or the compound may be an electride $Na^+_3(N_2)_4 \cdot 3e^-$, with electrons serving as anions like in some subnitrides (*e.g.* $[Ca_2N]^{+} \cdot e^-$).[51] A more unlikely scenario is that Na_3N_8 is a van der Waals compound without a charge transfer from sodium to nitrogen atoms. Similar considerations are valid for NaN_2 too. The first clue on the bonding situation comes from the analysis of interatomic nitrogen-nitrogen distances. Assuming the complete charge transfer from sodium to nitrogen atoms, the N-N bond orders in Na_3N_8 and NaN_2 should be 2.625 and 2.5, respectively. Therefore, in this case N-N distances should be only slightly longer than the triple N≡N bond.

Indeed, the interatomic nitrogen-nitrogen distances in Na_3N_8 and in NaN_2 (1.147 and 1.161 Å) are in a very good agreement with the formal N-N bond orders and clearly follow the trend d_{NN}(N≡N) < d_{NN}(Na_3N_8) < d_{NN} (NaN_2) < d_{NN}(diazenides) < d_{NN} (pernitrides). We note here that N-N dimers are very incompressible. For instance the N-N single bond length variation in ReN_2 between 0 and 42 GPa is about 0.05Å[15], while higher-order N-N bonds are expected to be even more incompressible. Therefore, for qualitative purposes, it is justified to compare N-N distances in compounds at slightly different pressures. The elongation of N-N distances in Na_3N_8 and in NaN_2 compared to N≡N suggests that charge transfer occurs in both compounds and the electrons are delocalized between nitrogen *p*-states, implying the metallic character of both compounds, which agrees with the observed black metallic color of the samples. In order to get a deeper insight into the bonding nature, we have performed electronic structure calculations that confirmed that both compounds are metallic (Figure 4) and the main contributions of bands at the Fermi level comes from the N 2*p* states.

Hitherto, several uncommon diazenides such as $(Sr^{2+})_8(N^{3-})_4([N_2]^{2-}) \cdot 2e^-$ or $(Li^+)_2(Ca^{2+})_3([N_2]^{2-})_3 \cdot 3e^-$ were synthesized at high-pressure conditions.[52,53] These compounds contain diazenide anions $[N_2]^{2-}$ and the delocalized electrons responsible for their metallic properties. By analogy with subnitrides such as $(Ba^{2+})_3(N^{3-}) \cdot 3e$, these compounds were called subdiazenides. On the contrary, both NaN_2 and Na_3N_8 may be considered as undercharged diazenides. Dinitrides with undercharged diazenide anions $[N_2]^-$ were recently reported in Li-N and Cu-N systems. Laniel *et al*. synthesized LiN_2 in a reaction between Li_3N and nitrogen at 10.5 GPa, while CuN_2 was synthesized from elements at ~50 GPa.[10] Both compounds have hexagonal NiAs *P*6$_3$/*mmc* structure type with N-N distances of ~1.2 Å. Undercharged $[N_2]^-$ diazenide groups are also present in Hf_2N_{11} compound synthesized at 1 Mbar.[20]

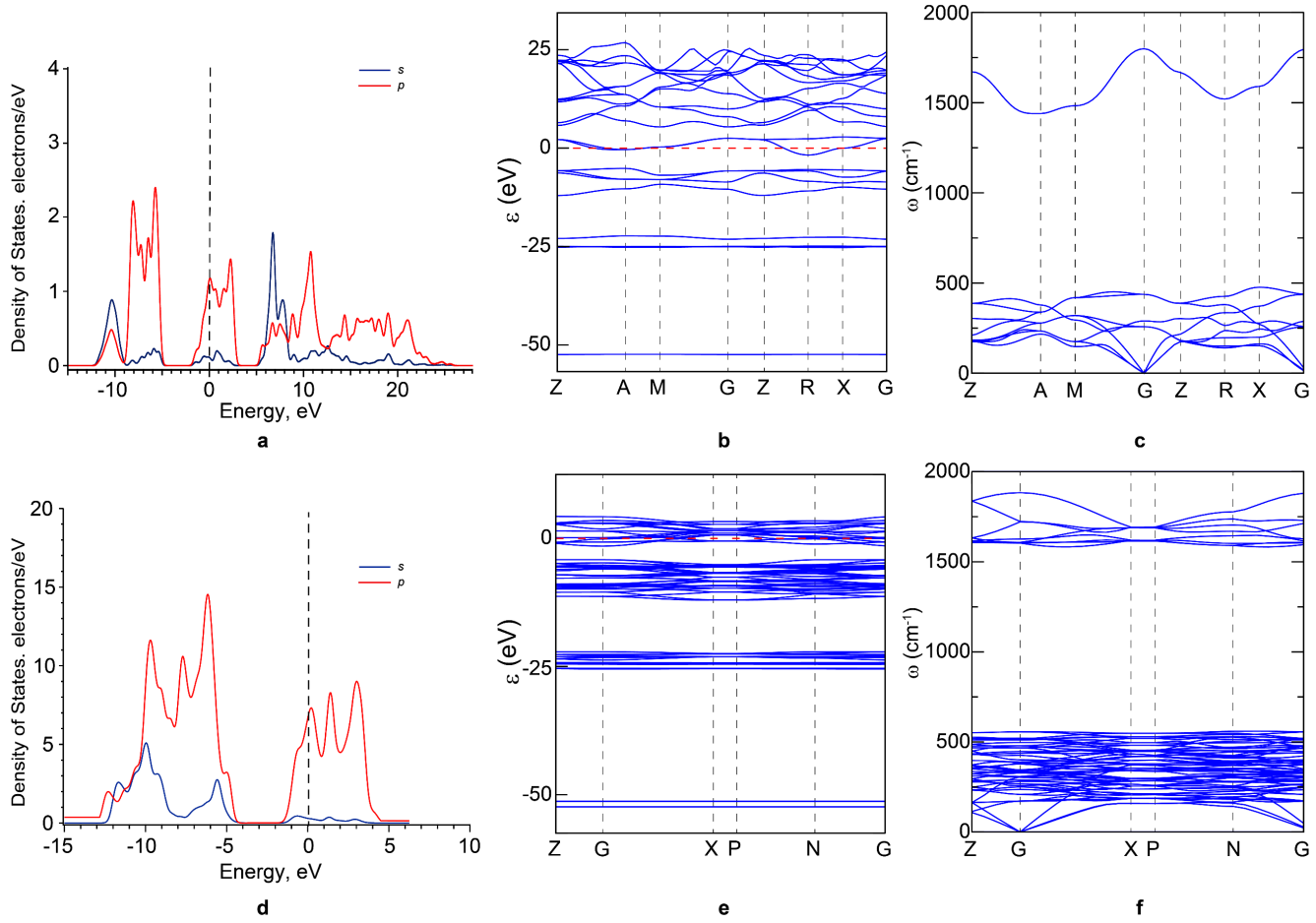

Figure 4. (a) Electron density of states, (b) band structure, and (c) phonon dispersion of NaN_2 at 4 GPa. (d) Electron density of states, (e) band structure, and (f) phonon dispersion of Na_3N_8 at 28 GPa.

An unprecedented example of Na_3N_8 demonstrates that $[N_2]$ units with non-integer formal charge exist. The $[N_2]$ unit may therefore serve as a versatile electron acceptor in solid-state chemistry and may exist not only in compounds with simple AB_2 or A_2B_2 stoichiometries.

Phonon dispersion calculations show that Na_3N_8 is dynamically stable at 28 GPa (Figure 4), but it becomes unstable at lower pressures as indicated by the appearance of imaginary phonon frequencies near the Z-point (Figure S7), which agrees with our experimental findings. We have also constructed a part of the convex hull diagram, showing the relative stabilities of the experimental Na-N phases in the vicinity of N:Na ratio 3:1 (Figure S8). At low pressure (4 GPa), *P*4/*mmm* NaN_2 phase is dynamically and thermodynamically stable. Interestingly, the most common Na-N phase NaN_3 emerges here as the least stable phase. At the first glance this seems counterintuitive, but in fact this compound is a metastable phase at standard conditions too: it has positive standard Gibbs free energy of formation $\Delta_f G^o$ = 93.7 kJ/mol.[54] NaN_3 is kinetically stable at ambient conditions with an activation barrier of ~150 kJ/mol for its decomposition reaction that requires breaking nitrogen-nitrogen bonds in the azide anion.[55] The decomposition of NaN_2 does not have this requirement and we can assume that the activation barrier of NaN_2 decomposition is substantially lower than that of NaN_3. That is why NaN_2 could not be preserved at ambient conditions but leaves a room for its low-temperature kinetic stabilization.

The formation of NaN_2 also agrees with the theoretical studies of Steele and Oleynik, who predicted *P*4/*mmm* NaN_2 in the Na-N system.[47] Our calculation of the convex hull diagram at 28 GPa shows that NaN_2 with *Cmmm* symmetry emerges as the thermodynamically stable phase (in agreement with Ref. [47]), while Na_3N_8 is slightly metastable (but is on the hull within the accuracy of the calculations). The calculations of Steele and Oleynik considered Na_xN_y structures having up to 16 atoms in the unit cell and this could explain why Na_3N_8, containing 44 atoms in the unit cell (22 atoms in the primitive cell) was not predicted. The existence of Na_3N_8 may have a consequence on the calculated stability regions of predicted NaN_5, and Na_2N_5 compounds.[47]

Conclusions

To conclude, in this study we discovered that pressure-temperature induced decomposition of sodium azide NaN_3 leads to two novel compounds Na_3N_8 and NaN_2. The studied reaction flow can be summarized by Scheme 1:

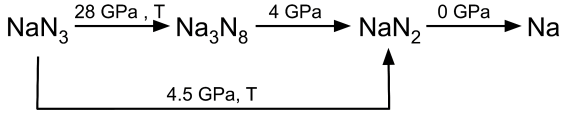

Scheme 1. Summary of pressure-temperature induced reactions in the Na-N system studied in this communication.

The dinitrogen units in NaN_2 and Na_3N_8 have formal charges of -1 and -0.75 respectively. N_2 unit is therefore the unique structural species that can accommodate a range of possible

formal charges including non-integer ones. This opens a new class of solid-state compounds containing homonuclear dinitrogen anions and having various compositions. It is likely that compounds with M_3N_8 stoichiometry may be found for group 2 metals with similar ionic radii as Na^+ (especially Ca and Sr). Replacing Na by the alkaline-earth metal in Na_3N_8 would lead to compounds $M^{II}_3N_8$ with $[N_2]^{1.5-}$.

Azides and NaN_3 in particular are often used in a synthesis of nitrides,[56–60] where they are commonly considered as solid sources of nitrogen, taking in account their ambient-pressure decomposition route ($2NaN_3 \rightarrow 2Na + 3N_2$). Our study shows that sodium azide can be already decomposed at 4 GPa, which results in the formation of activated $[N_2]^-$ species together with molecular N_2 and this mechanism may play a crucial role for the high-pressure solid-state metathesis synthetic approach that recently became widespread for the synthesis of nitrides.[61–63] The formation of stable Na_3N_8 compound with a very unexpected stoichiometry is an important indication that theoretical calculations, which became widespread in the high-pressure community[64,65] should always include variable-stoichiometry search and should not limit the unit cell contents to a few atoms for the sake of the computation time. Therefore, these experiments revealing unexpected compositions are an important contribution for the adjustments of computational strategies.

ASSOCIATED CONTENT

Supporting Information.
Crystallographic information files for Na_3N_8 and NaN_2. Details of structure refinement, powder diffraction patterns, Raman spectra. This material is available free of charge via the Internet at http://pubs.acs.org.

AUTHOR INFORMATION

Corresponding Author

* Maxim Bykov. maks.byk@gmail.com

Author Contributions

The manuscript was written through contributions of all authors. All authors have given approval to the final version of the manuscript.

Funding Sources

Research was sponsored by the Army Research Office and was accomplished under the Cooperative Agreement Number W911NF-19-2-0172.

ACKNOWLEDGMENT

Parts of this research were carried out at the Extreme Conditions Beamline (P02.2) at DESY, a member of Helmholtz Association (HGF). Portions of this work were performed at HPCAT (Sector 16), Advanced Photon Source (APS), Argonne National Laboratory. HPCAT operations are supported by DOE-NNSA's Office of Experimental Sciences. Raman spectroscopy experiments were performed at GeoSoilEnviroCARS (The University of Chicago, Sector 13), Advanced Photon Source (APS), Argonne National Laboratory. GeoSoilEnviroCARS is supported by the National Science Foundation - Earth Sciences (EAR - 1634415) and Department of Energy- GeoSciences (DE-FG02-94ER14466). The Advanced Photon Source is a U.S. Department of Energy (DOE) Office of Science User Facility operated for the DOE Office of Science by Argonne National Laboratory under Contract No. DE-AC02-06CH11357.

ABBREVIATIONS

XRD, X-ray diffraction; DAC, diamond anvil cell

REFERENCES

(1) Shaver, M. P.; Fryzuk, M. D. Activation of Molecular Nitrogen: Coordination, Cleavage and Functionalization of N2 Mediated By Metal Complexes. *Adv. Synth. Catal.* **2003**, *345* (910), 1061–1076. https://doi.org/10.1002/adsc.200303081.

(2) Crossland, J. L.; Tyler, D. R. Iron–Dinitrogen Coordination Chemistry: Dinitrogen Activation and Reactivity. *Coord. Chem. Rev.* **2010**, *254* (17–18), 1883–1894. https://doi.org/10.1016/j.ccr.2010.01.005.

(3) Yandulov, D. V.; Schrock, R. R. Catalytic Reduction of Dinitrogen to Ammonia at a Single Molybdenum Center. *Science* **2003**, *301* (5629), 76–78. https://doi.org/10.1126/science.1085326.

(4) Auffermann, G.; Prots, Y.; Kniep, R. SrN and SrN2: Diazenides by Synthesis under High N2-Pressure. *Angew. Chemie Int. Ed.* **2001**, *40* (3), 547–549. https://doi.org/10.1002/1521-3773(20010202)40:3<547::AID-ANIE547>3.0.CO;2-X.

(5) Vajenine, G. V.; Auffermann, G.; Prots, Y.; Schnelle, W.; Kremer, R. K.; Simon, A.; Kniep, R. Preparation, Crystal Structure, and Properties of Barium Pernitride, BaN2. *Inorg. Chem.* **2001**, *40* (19), 4866–4870. https://doi.org/10.1021/IC010263+.

(6) Schneider, S. B.; Frankovsky, R.; Schnick, W. Synthesis of Alkaline Earth Diazenides $M_{AE}N_2$ (M_{AE} = Ca, Sr, Ba) by Controlled Thermal Decomposition of Azides under High Pressure. *Inorg. Chem.* **2012**, *51* (4), 2366–2373. https://doi.org/10.1021/ic2023677.

(7) Schneider, S. B.; Frankovsky, R.; Schnick, W. High-Pressure Synthesis and Characterization of the Alkali Diazenide Li_2N_2. *Angew. Chemie Int. Ed.* **2012**, *51* (8), 1873–1875. https://doi.org/10.1002/anie.201108252.

(8) Bhadram, V. S.; Kim, D. Y.; Strobel, T. A. High-Pressure Synthesis and Characterization of Incompressible Titanium Pernitride. *Chem. Mater.* **2016**, *28* (6), 1616–1620. https://doi.org/10.1021/acs.chemmater.6b00042.

(9) Niwa, K.; Fukui, R.; Terabe, T.; Kawada, T.; Kato, D.; Sasaki, T.; Soda, K.; Hasegawa, M. High-Pressure Synthesis and Phase Stability of Nickel Pernitride. *Eur. J. Inorg. Chem.* **2019**, *2019* (33), 3753–3757. https://doi.org/10.1002/ejic.201900489.

(10) Binns, J.; Donnelly, M. E.; Pena-Alvarez, M.; Wang, M.; Gregoryanz, E.; Hermann, A.; Dalladay-Simpson, P.; Howie, R. T. Direct Reaction between Copper and Nitrogen at High Pressures and Temperatures. *J. Phys. Chem. Lett.* **2019**, *10* (5), 1109–1114. https://doi.org/10.1021/acs.jpclett.9b00070.

(11) Niwa, K.; Suzuki, K.; Muto, S.; Tatsumi, K.; Soda, K.; Kikegawa, T.; Hasegawa, M. Discovery of the Last Remaining Binary Platinum-Group Pernitride RuN_2. *Chem. - A Eur. J.* **2014**, *20* (43), 13885–13888. https://doi.org/10.1002/chem.201404165.

(12) Niwa, K.; Dzivenko, D.; Suzuki, K.; Riedel, R.; Troyan, I.; Eremets, M.; Hasegawa, M. High Pressure Synthesis of Marcasite-Type Rhodium Pernitride. *Inorg. Chem.* **2014**, *53* (2), 697–699. https://doi.org/10.1021/ic402885k.

(13) Bykov, M.; Yusenko, K. V.; Bykova, E.; Pakhomova, A.; Kraus, W.; Dubrovinskaia, N.; Dubrovinsky, L. Synthesis of Arsenopyrite-Type Rhodium Pernitride RhN 2 from a Single-Source Azide Precursor. *Eur. J. Inorg. Chem.* **2019**, *2019* (32), 3667–3671. https://doi.org/10.1002/ejic.201900488.

(14) Crowhurst, J. C.; Goncharov, A. F.; Sadigh, B.; Zaug, J. M.; Aberg, D.; Meng, Y.; Prakapenka, V. B. Synthesis and Characterization of Nitrides of Iridium and Palladium. *J. Mater. Res.* **2008**, *23* (01), 1–5. https://doi.org/10.1557/JMR.2008.0027.

(15) Bykov, M.; Chariton, S.; Fei, H.; Fedotenko, T.; Aprilis, G.; Ponomareva, A. V.; Tasnádi, F.; Abrikosov, I. A.; Merle, B.; Feldner, P.; et al. High-Pressure Synthesis of Ultraincompressible Hard Rhenium Nitride Pernitride Re2(N2)(N)2 Stable at Ambient Conditions. *Nat. Commun.* **2019**, *10* (1), 2994. https://doi.org/10.1038/s41467-019-10995-3.

(16) Crowhurst, J. C.; Goncharov, A. F.; Sadigh, B.; Evans, C. L.; Morral, P. G.; Ferreira, J. L.; Nelson, A. J. Synthesis and Characterization of the Nitrides of Platinum and Iridium. *Science* **2006**, *311* (5765), 1275–1278. https://doi.org/10.1126/science.1121813.

(17) Young, A. F.; Sanloup, C.; Gregoryanz, E.; Scandolo, S.; Hemley, R. J.; Mao, H. Synthesis of Novel Transition Metal Nitrides IrN_2 and OsN_2. *Phys. Rev. Lett.* **2006**, *96* (15), 155501. https://doi.org/10.1103/PhysRevLett.96.155501.

(18) Bykov, M.; Bykova, E.; Aprilis, G.; Glazyrin, K.; Koemets, E.; Chuvashova, I.; Kupenko, I.; McCammon, C.; Mezouar, M.;

Prakapenka, V.; et al. Fe-N System at High Pressure Reveals a Compound Featuring Polymeric Nitrogen Chains. *Nat. Commun.* **2018**, *9* (1), 2756. https://doi.org/10.1038/s41467-018-05143-2.

(19) Bykov, M.; Khandarkhaeva, S.; Fedotenko, T.; Sedmak, P.; Dubrovinskaia, N.; Dubrovinsky, L. Synthesis of FeN 4 at 180 GPa and Its Crystal Structure from a Submicron-Sized Grain. *Acta Crystallogr. Sect. E Crystallogr. Commun.* **2018**, *74*, 1392–1395. https://doi.org/10.1107/S2056989018012161.

(20) Bykov, M.; Chariton, S.; Bykova, E.; Khandarkhaeva, S.; Fedotenko, T.; Ponomareva, A. V.; Tidholm, J.; Tasnádi, F.; Abrikosov, I. A.; Sedmak, P.; et al. High‐Pressure Synthesis of Metal–Inorganic Frameworks Hf 4 N 20 ·N 2 , WN 8 ·N 2 , and Os 5 N 28 ·3 N 2 with Polymeric Nitrogen Linkers. *Angew. Chemie Int. Ed.* **2020**, *59* (26), 10321–10326. https://doi.org/10.1002/anie.202002487.

(21) Laniel, D.; Winkler, B.; Koemets, E.; Fedotenko, T.; Bykov, M.; Bykova, E.; Dubrovinsky, L.; Dubrovinskaia, N. Synthesis of Magnesium-Nitrogen Salts of Polynitrogen Anions. *Nat. Commun.* **2019**, *10* (1), 4515. https://doi.org/10.1038/s41467-019-12530-w.

(22) Bykov, M.; Bykova, E.; Koemets, E.; Fedotenko, T.; Aprilis, G.; Glazyrin, K.; Liermann, H.-P.; Ponomareva, A. V.; Tidholm, J.; Tasnádi, F.; et al. High-Pressure Synthesis of a Nitrogen-Rich Inclusion Compound ReN8·xN2 with Conjugated Polymeric Nitrogen Chains. *Angew. Chemie Int. Ed.* **2018**, *57* (29), 9048–9053. https://doi.org/10.1002/anie.201805152.

(23) Steele, B. A.; Stavrou, E.; Crowhurst, J. C.; Zaug, J. M.; Prakapenka, V. B.; Oleynik, I. I. High-Pressure Synthesis of a Pentazolate Salt. *Chem. Mater.* **2017**, *29* (2), 735–741. https://doi.org/10.1021/acs.chemmater.6b04538.

(24) Laniel, D.; Weck, G.; Gaiffe, G.; Garbarino, G.; Loubeyre, P. High-Pressure Synthesized Lithium Pentazolate Compound Metastable under Ambient Conditions. *J. Phys. Chem. Lett.* **2018**, *9* (7), 1600–1604. https://doi.org/10.1021/acs.jpclett.8b00540.

(25) Pulham; Millar; Barry; Marshall. Structural Characterization of Sodium Azide and Sodium Bifluoride at High Pressures. *Zeitschrift für Krist. Cryst. Mater.* **2014**, *229* (3), 259–275. https://doi.org/10.1515/zkri-2013-1660.

(26) Zhu, H.; Zhang, F.; Ji, C.; Hou, D.; Wu, J.; Hannon, T.; Ma, Y. Pressure-Induced Series of Phase Transitions in Sodium Azide Pressure-Induced Series of Phase Transitions in Sodium Azide. *J. Appl. Phys.* **2016**, *113* (2013), 033511. https://doi.org/10.1063/1.4776235.

(27) Eremets, M. I.; Popov, M. Y.; Trojan, I. A.; Denisov, V. N.; Boehler, R.; Hemley, R. J. Polymerization of Nitrogen in Sodium Azide. *J. Chem. Phys.* **2004**, *120* (22), 10618–10623. https://doi.org/10.1063/1.1718250.

(28) Zhang, M.; Yin, K.; Zhang, X.; Wang, H.; Li, Q.; Wu, Z. Structural and Electronic Properties of Sodium Azide at High Pressure: A First Principles Study. *Solid State Commun.* **2013**, *161*, 13–18. https://doi.org/10.1016/j.ssc.2013.01.032.

(29) Peiris, S. M.; Russell, T. P. Photolysis of Compressed Sodium Azide (NaN 3) as a Synthetic Pathway to Nitrogen Materials. *J. Phys. Chem. A* **2003**, *107* (6), 944–947. https://doi.org/10.1021/jp025963u.

(30) Holtgrewe, N.; Lobanov, S. S.; Mahmood, M. F.; Goncharov, A. F. Photochemistry within Compressed Sodium Azide. *J. Phys. Chem. C* **2016**, *120* (49), 28176–28185. https://doi.org/10.1021/acs.jpcc.6b09103.

(31) Kantor, I.; Prakapenka, V.; Kantor, A.; Dera, P.; Kurnosov, A.; Sinogeikin, S.; Dubrovinskaia, N.; Dubrovinsky, L. BX90: A New Diamond Anvil Cell Design for X-Ray Diffraction and Optical Measurements. *Rev. Sci. Instrum.* **2012**, *83* (12), 125102. https://doi.org/10.1063/1.4768541.

(32) Boehler, R. New Diamond Cell for Single-Crystal x-Ray Diffraction. *Rev. Sci. Instrum.* **2006**, *77* (11), 115103. https://doi.org/10.1063/1.2372734.

(33) Liermann, H.-P.; Konôpková, Z.; Morgenroth, W.; Glazyrin, K.; Bednarčik, J.; McBride, E. E.; Petitgirard, S.; Delitz, J. T.; Wendt, M.; Bican, Y.; et al. The Extreme Conditions Beamline P02.2 and the Extreme Conditions Science Infrastructure at PETRA III. *J. Synchrotron Radiat.* **2015**, *22* (4), 908–924. https://doi.org/10.1107/S1600577515005937.

(34) Sheldrick, G. M. SHELXT – Integrated Space-Group and Crystal-Structure Determination. *Acta Crystallogr. Sect. A Found. Adv.* **2015**, *71* (1), 3–8. https://doi.org/10.1107/S2053273314026370.

(35) Sheldrick, G. M. Crystal Structure Refinement with SHELXL. *Acta Crystallogr. Sect. C Struct. Chem.* **2015**, *71* (1), 3–8. https://doi.org/10.1107/S2053229614024218.

(36) Prescher, C.; Prakapenka, V. B. DIOPTAS: A Program for Reduction of Two-Dimensional X-Ray Diffraction Data and Data Exploration. *High Press. Res.* **2015**, *35* (3), 223–230. https://doi.org/10.1080/08957959.2015.1059835.

(37) Petricek, V.; Dusek, M.; Palatinus, L. Crystallographic Computing System JANA2006: General Features. *Zeitschrift für Krist.* **2014**, *229* (5), 345–352.

(38) Holtgrewe, N.; Greenberg, E.; Prescher, C.; Prakapenka, V. B.; Goncharov, A. F. Advanced Integrated Optical Spectroscopy System for Diamond Anvil Cell Studies at GSECARS. *High Press. Res.* **2019**, *39* (3), 457–470. https://doi.org/10.1080/08957959.2019.1647536.

(39) Hamann, D. R.; Schlüter, M.; Chiang, C. Norm-Conserving Pseudopotentials. *Phys. Rev. Lett.* **1979**, *43* (20), 1494–1497. https://doi.org/10.1103/PhysRevLett.43.1494.

(40) Segall, M. D.; Lindan, P. J. D.; Probert, M. J.; Pickard, C. J.; Hasnip, P. J.; Clark, S. J.; Payne, M. C. First-Principles Simulation: Ideas, Illustrations and the CASTEP Code. *J. Phys. Condens. Matter* **2002**, *14* (11), 2717–2744. https://doi.org/10.1088/0953-8984/14/11/301.

(41) Perdew, J. P.; Burke, K.; Ernzerhof, M. Generalized Gradient Approximation Made Simple. *Phys. Rev. Lett.* **1996**, *77* (18), 3865–3868. https://doi.org/10.1103/PhysRevLett.77.3865.

(42) Tkatchenko, A.; Scheffler, M. Accurate Molecular Van Der Waals Interactions from Ground-State Electron Density and Free-Atom Reference Data. *Phys. Rev. Lett.* **2009**, *102* (7), 073005. https://doi.org/10.1103/PhysRevLett.102.073005.

(43) Monkhorst, H. J.; Pack, J. D. Special Points for Brillouin-Zone Integrations. *Phys. Rev. B* **1976**, *13* (12), 5188–5192. https://doi.org/10.1103/PhysRevB.13.5188.

(44) Refson, K.; Tulip, P. R.; Clark, S. J. Variational Density-Functional Perturbation Theory for Dielectrics and Lattice Dynamics. *Phys. Rev. B* **2006**, *73* (15), 155114. https://doi.org/10.1103/PhysRevB.73.155114.

(45) Segall, M. D.; Pickard, C. J.; Shah, R.; Payne, M. C. Population Analysis in Plane Wave Electronic Structure Calculations. *Mol. Phys.* **1996**, *89* (2), 571–577. https://doi.org/10.1080/002689796173912.

(46) Zhang, W.; Wang, K.; Li, J.; Lin, Z.; Song, S.; Huang, S.; Liu, Y.; Nie, F.; Zhang, Q. Stabilization of the Pentazolate Anion in a Zeolitic Architecture with Na 20 N 60 and Na 24 N 60 Nanocages. *Angew. Chemie Int. Ed.* **2018**, *57* (10), 2592–2595. https://doi.org/10.1002/anie.201710602.

(47) Steele, B. A.; Oleynik, I. I. Sodium Pentazolate: A Nitrogen Rich High Energy Density Material. *Chem. Phys. Lett.* **2016**, *643*, 21–26. https://doi.org/10.1016/j.cplett.2015.11.008.

(48) Hanfland, M.; Loa, I.; Syassen, K. Sodium under Pressure: Bcc to Fcc Structural Transition and Pressure-Volume Relation to 100 GPa. *Phys. Rev. B - Condens. Matter Mater. Phys.* **2002**, *65* (18), 1841091–1841098. https://doi.org/10.1103/PhysRevB.65.184109.

(49) O'Keeffe, M.; Eddaoudi, M.; Li, H.; Reineke, T.; Yaghi, O. M. Frameworks for Extended Solids: Geometrical Design Principles. *J. Solid State Chem.* **2000**, *152* (1), 3–20. https://doi.org/10.1006/jssc.2000.8723.

(50) Kovács, A. Coordination of N2 Ligands to Lanthanum: The Complexes La (N2)1–8. *Struct. Chem.* **2018**, *29* (6), 1825–1837. https://doi.org/10.1007/s11224-018-1177-2.

(51) Lee, K.; Kim, S. W.; Toda, Y.; Matsuishi, S.; Hosono, H. Dicalcium Nitride as a Two-Dimensional Electride with an Anionic Electron Layer. *Nature* **2013**, *494* (7437), 336–340. https://doi.org/10.1038/nature11812.

(52) Prots, Y.; Auffermann, G.; Tovar, M.; Kniep, R. Sr4N3: A Hitherto Missing Member in the Nitrogen Pressure Reaction Series Sr2N→Sr4N3→SrN→SrN2. *Angew. Chemie Int. Ed.* **2002**, *41* (13), 2288–2290. https://doi.org/10.1002/1521-3773(20020703)41:13<2288::AID-ANIE2288>3.0.CO;2-I.

(53) Schneider, S. B.; Seibald, M.; Deringer, V. L.; Stoffel, R. P.; Frankovsky, R.; Friederichs, G. M.; Laqua, H.; Duppel, V.; Jeschke, G.; Dronskowski, R.; et al. High-Pressure Synthesis and Characterization of Li2Ca 3[N2]3 - An Uncommon Metallic Diazenide with [N2]2- Ions. *J. Am. Chem. Soc.* **2013**, *135* (44), 16668–16679. https://doi.org/10.1021/ja408816t.

(54) Patnaik, P. *Handbook of Inorganic Chemicals*; McGraw-Hill, 2002. https://doi.org/10.5860/choice.40-6428.
(55) Potvin, H.; Back, M. H. A Study of the Decomposition of Sodium Azide Using Differential Thermal Analysis. *Can. J. Chem.* **1973**, *51* (2), 183–186. https://doi.org/10.1139/v73-028.
(56) Kloß, S. D.; Schnick, W. Nitridophosphates: A Success Story of Nitride Synthesis. *Angew. Chemie Int. Ed.* **2019**, *58* (24), 7933–7944. https://doi.org/10.1002/anie.201812791.
(57) Karau, F. W.; Schnick, W. High-Pressure Synthesis and X-Ray Powder Structure Determination of the Nitridophosphate. *J. Solid State Chem.* **2005**, *178* (1), 135–141. https://doi.org/10.1016/j.jssc.2004.10.034.
(58) Karau, F. W.; Seyfarth, L.; Oeckler, O.; Senker, J.; Landskron, K.; Schnick, W. The Stuffed Framework Structure of SrP2N4: Challenges to Synthesis and Crystal Structure Determination. *Chem. - A Eur. J.* **2007**, *13* (24), 6841–6852. https://doi.org/10.1002/chem.200700216.
(59) Landskron, K.; Irran, E.; Schnick, W. High-Temperature High-Pressure Synthesis of the Highly Condensed Nitridophosphates NaP4N7, KP4N7, RbP4N7, and CsP4N7 and Their Crystal-Structure Determinations by X-Ray Powder Diffraction. *Chem. - A Eur. J.* **1999**, *5* (9), 2548–2553. https://doi.org/10.1002/(SICI)1521-3765(19990903)5:9<2548::AID-CHEM2548>3.3.CO;2-N.
(60) Gillan, E. G.; Kaner, R. B. Rapid Solid-State Synthesis of Refractory Nitrides. *Inorg. Chem.* **1994**, *33* (25), 5693–5700. https://doi.org/10.1021/ic00103a015.
(61) Lei, L.; Zhang, L. Recent Advance in High-Pressure Solid-State Metathesis Reactions. *Matter Radiat. Extrem.* **2018**, *3* (3), 95–103. https://doi.org/10.1016/j.mre.2017.12.003.
(62) Kawamura, F.; Yusa, H.; Taniguchi, T. Synthesis of Hexagonal Phases of WN and W 2.25 N 3 by High-Pressure Metathesis Reaction. *J. Am. Ceram. Soc.* **2018**, *101* (2), 949–956. https://doi.org/10.1111/jace.15235.
(63) Kawamura, F.; Yamada, N.; Cao, X.; Imai, M.; Taniguchi, T. The Bandgap of ZnSnN 2 with a Disordered-Wurtzite Structure. *Jpn. J. Appl. Phys.* **2019**, *58* (SC), SC1034. https://doi.org/10.7567/1347-4065/ab0ace.
(64) Zhu, S.; Peng, F.; Liu, H.; Majumdar, A.; Gao, T.; Yao, Y. Stable Calcium Nitrides at Ambient and High Pressures. *Inorg. Chem.* **2016**, *55* (15), 7550–7555. https://doi.org/10.1021/acs.inorgchem.6b00948.
(65) Peng, F.; Han, Y.; Liu, H.; Yao, Y. Exotic Stable Cesium Polynitrides at High Pressure. *Sci. Rep.* **2015**, *5*, 16902. https://doi.org/10.1038/srep16902.

SYNOPSIS

Here using a controlled decomposition of sodium azide NaN_3 at high pressure conditions two novel compounds $Na_3(N_2)_4$ and NaN_2 were synthesized. Both contain dinitrogen anions. NaN_2 might be the common intermediate in high-pressure solid-state metathesis reactions where NaN_3 is used as a source of nitrogen. $Na_3(N_2)_4$ opens a new class of compounds, where $[N_2]$ units accommodate a non-integer formal charge.

For Table of Contents Only